

Extended quark mass density- and temperature- dependent model and the deconfinement phase transition

Wei Liang Qian*

Department of Physics, Fudan University, Shanghai 200433, P.R.China

Ru-Keng Su[†]

China Center of Advanced Science and Technology (World Laboratory),

P. O. Box 8730, Beijing 100080, P.R.China and

Department of Physics, Fudan University, Shanghai 200433, P.R.China

Abstract

An extended quark mass density- and temperature- dependent model which includes the couplings between quarks and the σ -mesons, ω -mesons is suggested. The MIT bag boundary constrain has been given up and the interactions between quarks and mesons are extended to the whole free space. We show that the present model is successful to describe both the saturation properties and the deconfinement phase transition of nuclear matter. When the effective nucleon masses vanish and the bag radius tends to infinite, the quark deconfinement phase transition takes place. The corresponding QGP phase diagram is addressed.

* wlqian@fudan.edu.cn

[†] rksu@fudan.ac.cn

I. INTRODUCTION

Because of the non-perturbative properties of QCD at low energy regions, it is very difficult to study nuclear system by using QCD as a fundamental theory directly. Various phenomenological models based either on hadron degree of freedom or quark degree of freedom have been suggested. The quark-meson coupling (QMC) model, first proposed by Guichon[1], which describes nuclear matter as a collection of non-overlapping MIT bags, scalar σ meson and vector ω meson is one of such successful candidates. The quarks inside the MIT bag couple with the scalar σ meson and vector ω meson self-consistently. By means of this model and the mean field approximation, many dynamical and thermal properties of nucleon systems and hyperon systems have been studied both at zero temperature and finite temperature[2, 3, 4, 5, 6, 7, 8].

Although QMC model is successful for describing the physical properties of nuclear system, many shortcomings arise when one use this model to discuss the quark deconfinement. The first difficulty comes from that this is a permanent quark confinement model. The nucleon corresponds to a MIT bag and the mechanism of quark confinement in MIT bag model being that the normal flow of quark current is zero at the bag surface. This boundary condition can not be changed by temperature and density. The second difficulty arises from the many-body calculations. If we hope to do the nuclear many-body calculations beyond mean field approximation by quantum field theory, it is essential to find the propagators of quark, σ meson and ω meson respectively. But the constrain of MIT bag boundary condition and the interaction between quarks and mesons limited within the bag regions present obstacles to get the corresponding propagators in free space.

On the other hand, another effective model, namely, the quark mass density- dependent (QMDD) model, was suggested by Fowler, Raha and Weiner[9]. According to this model, the masses of u, d quarks and strange s quark (together with the corresponding anti-quarks) are given by

$$m_q = \frac{B}{n_Q} \quad (q = u, d, \bar{u}, \bar{d}) \quad (1)$$

$$m_{s,\bar{s}} = m_{s0} + \frac{B}{n_Q} \quad (2)$$

where B is the vacuum energy density inside the bag and n_Q is the quark number density. The basic hypothesis Eqs.(1) and (2) corresponds to a quark confinement mechanism because

if quark goes to infinite, the volume of the system tends to infinite, n_Q approaches zero and m_q approaches to infinite. The infinite quark mass prevents the quark from going to infinite[10, 11]. This confinement mechanism is very similar to that of the MIT bag model. As was shown in ref.[10], the properties of strange matter in QMDD model are nearly the same as those obtained by the MIT bag model. Although the confinement mechanism is similar, the advantage of QMDD model is that it does not need to introduce a boundary condition to confine quark as that of the MIT bag model.

As was pointed by refs.[12, 13], if we use QMDD model to investigate the thermodynamical properties of nuclear system at finite temperature, many difficulties will emerge. For example, it cannot reproduce a correct lattice QCD phase diagram qualitatively because the masses of quarks, and then the temperature tends to infinite when $n_B \rightarrow 0$ [12]. The reason is that the confinement mechanism of QMDD model is still permanent. To overcome this difficulty, in a series of our pervious papers[11, 12, 13, 14, 15, 16], we suggested a quark mass density- and temperature- dependent (QMDDT) model. Instead of the permanent MIT quark confinement mechanism, we employed the Friedberg-Lee (FL) soliton bag model. Since the confinement mechanism of FL model comes from the interaction between quarks and a nontopological scalar soliton field, and the spontaneously broken symmetry of the scalar field will be restored at a finite temperature, the soliton solution will disappear and the quark will deconfine at the critical temperature. In this nonpermanent quark confinement model, the vacuum energy density B equals the different value between the perturbative vacuum and physical vacuum, and it depends on temperature. Instead of Eqs.(1) and (2), we introduced[11, 12, 13, 14, 15, 16]

$$B(T) = B_0 \left[1 - \left(\frac{T}{T_c} \right)^2 \right] \quad 0 \leq T \leq T_c \quad (3)$$

$$B(T) = 0 \quad T > T_c \quad (4)$$

and

$$m_q = \frac{B_0}{n_Q} \left[1 - \left(\frac{T}{T_c} \right)^2 \right] \quad (q = u, d, \bar{u}, \bar{d}) \quad 0 \leq T \leq T_c \quad (5)$$

$$m_q = 0 \quad T > T_c \quad (6)$$

$$m_{s,\bar{s}} = m_{s0} + \frac{B_0}{n_Q} \left[1 - \left(\frac{T}{T_c} \right)^2 \right] \quad 0 \leq T \leq T_c \quad (7)$$

$$m_{s,\bar{s}} = m_{s0} \quad T > T_c \quad (8)$$

in QMDTD model. The masses of quarks not only depend on density but also on temperature. Obviously, the QMDTD model reduces to QMDD model at zero temperature. By means of the QMDTD model, the physical properties and the stability of strangelets[13], the dibaryon system[15] and the strange star[17, 18] at finite temperature have been studied and the results are fine.

Although the masses of quarks reflect the confinement characteristic in the QMDTD model, it is still an ideal quark gas model. If we hope to investigate the saturation properties and the deconfinement phase transition of nuclear matter, the quark-quark interaction must be taken into consideration. In ref.[16], a quark and non-linear scalar field coupling is introduced to improved QMDD model at zero temperature. We proved that many physical properties given by FL soliton bag model can be mimicked by the improved QMDD model.

This paper evolves from an attempt to extend our study to finite temperature. We will introduce the scalar σ meson, vector ω meson and the couplings between quarks (u, d) and σ meson, ω meson in the extended quark mass density- and temperature- dependent (EQMDTD) model. Our EQMDTD model is similar to that of Walecka model and QMC model. The basic differences between the EQMDTD model and the Walecka model are: (1)we replace the nucleon in Walecka model by quark in EQMDTD model; (2)rather than the structureless point-like nucleon in Walecka model, the nucleon corresponds to a "cluster", say, bag which consists three quarks with temperature- and density- dependent masses given by Eqs(5) and (6). Besides, the differences between the EQMDTD model and the QMC model are: (1)instead of the MIT bag in QMC model, we incorporate quarks with density- and temperature- dependent masses in EQMDTD model; (2)in place of the quark- σ quark- ω interactions restricted within the bag region in QMC model, the quark- σ , quark- ω interactions are spreaded to the whole free space, because the constraint of MIT bag boundary condition is discarded. Moreover, since our model are based on the FL model, the quark deconfinement phase transition can take place. we will address the behavior of the saturation and the deconfinement phase transition for EQMDTD model in this paper.

The organization of this paper is as follows. In the next section, we will give a brief description of EQMDTD model and the main formulae. Our numerical results will be presented in Section III. The last section is devoted to discussion and conclusion.

II. THE EQMDTD MODEL

The Lagrangian density of the EQMDTD model is

$$\mathcal{L} = \bar{\psi} [i\gamma^\mu \partial_\mu - m_q + (g_\sigma^q \sigma - g_\omega^q \gamma^\mu \omega_\mu)] \psi + \frac{1}{2} \partial_\mu \sigma \partial^\mu \sigma - \frac{1}{2} m_\sigma^2 \sigma^2 - \frac{1}{4} F_{\mu\nu} F^{\mu\nu} + \frac{1}{2} m_\omega^2 \omega_\mu \omega^\mu \quad (9)$$

where the quark mass m_q is given by Eqs.(5) and (6), m_σ , m_ω are the masses of σ and ω mesons, $F_{\mu\nu} = \partial_\mu \omega_\nu - \partial_\nu \omega_\mu$, g_σ^q and g_ω^q are the couplings between quark- σ meson and quark- ω meson respectively. We neglect the s quark in the following discussion.

The equation of motion for quark field is

$$[\gamma^\mu (i\partial_\mu + g_\omega^q \omega_\mu) - (m_q - g_\sigma^q \sigma)] \psi = 0 \quad (10)$$

Under mean field approximation, the effective quark mass m_q^* is given by

$$m_q^* = m_q - g_\sigma^q \bar{\sigma} \quad (11)$$

In nuclear matter, three quarks constitute a bag, say nucleon, and the effective nucleon mass is obtained from the bag energy and reads

$$M_N^* = E_{bag} = \sum_q E_q = \frac{4}{3} \gamma \pi R^3 \sum_{q=u,d} \sum_k \varepsilon_q(k) (f_q(k) + \bar{f}_q(k)) \quad (12)$$

where $\varepsilon_q(k) = \sqrt{m_q^{*2} + k^2}$ is the single particle energy, γ is the degeneracy, $f_q(k)$ and $\bar{f}_q(k)$ are the Fermi distributions of quark and anti-quark respectively

$$f_q(k) = \frac{1}{e^{\beta(\varepsilon_q(k) - \mu_q)} + 1} \quad (13)$$

$$\bar{f}_q(k) = \frac{1}{e^{\beta(\varepsilon_q(k) + \mu_q)} + 1} \quad (14)$$

The chemical potential μ_q of quark is given by

$$n_Q = \gamma \sum_{q=u,d} \sum_k (f_q(k) - \bar{f}_q(k)) \quad (15)$$

$$3 = \frac{4}{3} \pi R^3 n_Q \quad (16)$$

The bag radius R is determined by the equilibrium condition for the nucleon bag

$$\frac{\delta M_N^*}{\delta R} = 0 \quad (17)$$

In nuclear matter, the total energy density is given by[2]

$$\mathcal{E}_{matter} = \sum_{i=N,P} \frac{2}{(2\pi)^3} \int d^3k \sqrt{M_i^{*2} + k^2} (n_i(k) + \bar{n}_i(k)) + \frac{g_\omega^2}{2m_\omega^2} \rho_B^2 + \frac{1}{2} m_\sigma^2 \bar{\sigma}^2 \quad (18)$$

where ρ_B is the density of nuclear matter

$$\rho_B = \sum_i \frac{2}{(2\pi)^3} \int d^3k (n_i(k) + \bar{n}_i(k)) \quad (19)$$

$n_i(k)$ and $\bar{n}_i(k)$ are the Fermi distributions of nucleon and anti-nucleon respectively,

$$n_i(k) = \frac{1}{e^{\beta(\sqrt{M_N^{*2} + k^2} - \mu_i)} + 1} \quad (20)$$

$$\bar{n}_i(k) = \frac{1}{e^{\beta(\sqrt{M_N^{*2} + k^2} + \mu_i)} + 1} \quad (21)$$

μ_i is the chemical potential of the i th nucleon. In Eq.(18), g_ω is the coupling between nucleon and ω meson and it satisfies $g_\omega = 3g_\omega^q$. As that of QMC model[2, 3, 4, 5, 6, 7, 8] the scalar mean field of σ meson is determined by self-consistency condition

$$\left. \frac{\delta E_{matter}}{\delta \sigma} \right|_{\sigma=\bar{\sigma}} = 0 \quad (22)$$

which yields

$$\bar{\sigma} = -\frac{2}{m_\sigma^2 (2\pi)^3} \sum_{i=N,P} \int d^3k \frac{M_i^*}{\sqrt{M_i^{*2} + k^2}} \left(\frac{\partial M_i^*}{\partial \bar{\sigma}} \right)_{bag,T} (n_i(k) + \bar{n}_i(k)) \quad (23)$$

Eqs.(5),(9)-(20) form a complete set of equations and we can solve them numerically. Our numerical results will be shown in the next section.

III. RESULTS

Before numerical calculation, let us discuss the effective quark mass m_q^* carefully because this quantity affects our results directly. To take the medium effects into account, Jin and Jinnings suggested a modified QMC model[3] in which the bag parameter B depends on density. In EQMDTD model, based on FL model, the bag parameter B depends on temperature (Eq.(3)), and the quark mass m_q depends on quark density n_Q . As was shown in section I, this quark density dependence of m_q corresponds to a quark confinement mechanism only. The medium effect has not yet been considered. To exhibit the medium effects, instead of

$B = B(n_Q)$ in the modified QMC model, we introduce an ansatz that the effective coupling of quarks and σ meson g_σ^q is a function of quark density n_Q , which can be expanded as

$$g_\sigma^q = g_\sigma^{q(0)}/n_Q + g_\sigma^{q(1)}/n_Q^2 + g_\sigma^{q(2)}/n_Q^3 \quad (24)$$

Eq.(9) becomes

$$m_q^* = \frac{B_0 [1 - (T/T_c)^2] - (g_\sigma^{q(0)} + g_\sigma^{q(1)}/n_Q + g_\sigma^{q(2)}/n_Q^2)\bar{\sigma}}{n_Q} \quad (25)$$

In fact, the density- dependent couplings of $NN\pi$, $NN\rho$, $NN\sigma$ have been employed by many authors to discuss many different problems[19, 20, 21, 22, 23]. Eq.(24) is an extension to quark level only. The values of the adjusted parameters $g_\sigma^{q(0)}$, $g_\sigma^{q(1)}$ and $g_\sigma^{q(2)}$ will be determined below.

Now we discuss the parameters in EQMDTD model. Firstly, we choose $m_\omega = 783$ MeV, $m_\sigma = 509$ MeV as that of refs.[24, 25]; $T_c = 170$ MeV as the deconfinement temperature at zero baryon density. To fix the nucleon mass $M_N = 939$ MeV, we take $B_0 = 173$ MeVfm⁻³. Beside these parameters, there are still four parameters, namely, g_ω^q , $g_\sigma^{q(0)}$, $g_\sigma^{q(1)}$ and $g_\sigma^{q(2)}$ needed to be fixed. Obviously, the behavior at the saturation point and the deconfinement phase transition must be explained if EQMDTD model is successful. We see below that the quark deconfinement phase transition will take place at the point $M_N^* \rightarrow 0$ and bag radius $R \rightarrow \infty$. Therefore, we fix parameters g_ω^q , $g_\sigma^{q(0)}$, $g_\sigma^{q(1)}$ and $g_\sigma^{q(2)}$ by the condition that at zero temperature, binding energy $E = -15$ MeV, the ratio of the effective nucleon mass to the nucleon mass $M_N^*/M_N = 0.6$ at the saturation density $\rho_0 = 0.15$ fm⁻³, and the deconfinement phase transition takes place at $\rho_B = 10\rho_0$. We find

$$g_\sigma^{q(0)} = 5.93 fm^{-3}, \quad g_\sigma^{q(1)} = -0.747 fm^{-6}, \quad g_\sigma^{q(2)} = 0.035 fm^{-9}, \quad g_\omega^q = 4.23$$

Now we are in a position to do numerical calculations and the results are shown in Fig.1a- Fig.9b. In Fig.1a, we omit the contribution of σ -meson and ω -meson and depict the bag energy as a function of bag radius at different temperatures $T = 0, 30, 60, 100, 150, 170$ MeV respectively. In this specific case, the EQMDTD model reduces to the original QMDTD model without quark-meson interaction. Fig.1b is the same diagram as that of Fig.1a but that contribution of meson fields has been taken into consideration. We fix $\bar{\sigma} = 20$ MeV. It is found from Fig.1a and Fig.1b that the radius of the bag given by the minimum of the curve increases with increasing temperature. When $T < 100$ MeV, the bag radius varies merely

slightly with increasing temperature. This result is similar to that of the QMC model or the FL model. However, when the temperature approaches to the critical temperature t_c , the bag radius increases significantly.

Noting that the $\bar{\sigma}$ connects to the baryon density ρ_B by Eq.(23) directly, instead of ρ_B , we employ $\bar{\sigma}$ to show our results first. The curves of effective nuclear mass M^* vs. the mean field $\bar{\sigma}$ at different temperatures $T = 0, 30, 60, 100, 130, 160$ MeV are shown in Fig.2. We see that the effective nucleon mass decreases when $\bar{\sigma}$ increases. In particular, we find a very interesting phenomenon: when $\bar{\sigma}$ approaches to a fixed point $\bar{\sigma}_c$, M^* drops to zero rapidly. This fixed point $\bar{\sigma}_c$ decreases as the temperature increases. The result $M^* = 0$ means that the nucleon is dissolved and the quark deconfinement phase transition takes place. To show this phase transition more clearly, we draw the curves R vs. $\bar{\sigma}$ at different temperatures $T = 0, 30, 60, 100, 130, 160$ MeV in Fig.3. We see that at the same critical point $\bar{\sigma}_c$ shown by Fig.2, the bag radius R tends to infinite rapidly. This result confirms that this is indeed a critical point of deconfinement phase transition, because at this case quarks occupy the whole system. Similarly, for fixed $\bar{\sigma} = 0, 20, 40, 60, 70, 75$ MeV, we show M^* vs. T curves and R vs. T curves in Fig.4 and Fig.5 respectively. We see that for every curve, M^* drops to zero and R tends to infinite at a critical temperature t_c . The critical temperature t_c increases when $\bar{\sigma}_c$ decreases. These results exhibit that the quark deconfinement phase transition can be described by EQMDTD model naturally.

Now let us show the connection between $\bar{\sigma}_c$ and the baryon density ρ_B . Employing Eqs. (19) and (23), one can obtain the relation of $\bar{\sigma}$ and ρ_B . The result is shown in Fig.6. For a fixed temperature, $\bar{\sigma}$ is a monotonical function of ρ_B . It means that $\bar{\sigma}$ can play the same role as that of ρ_B . For example, M^* vs. $\bar{\sigma}$ curve has the same behavior as that of M^* vs. ρ_B curve. The curve in Fig.7 shows that when $\bar{\sigma}_c$ increases, the critical temperature t_c decreases. It corresponds to the result that when ρ_B^c increases, t_c decreases for the quark deconfinement phase transition. This is of course very reasonable. In fact, Fig.7 is the deconfinement phase diagram for EQMDTD model. It is very similar to that given by lattice calculation.

Now we turn to address the saturation properties of nuclear matter at low temperature and low density by using the EQMDTD model. Our results are shown in Fig.8, Fig.9a and Fig.9b. The curves of $\mathcal{E}_{matter}/\rho_B - M_N$ vs. ρ_B for different temperatures are shown in Fig.8 where the curve at $T = 0$ MeV refers to the saturation curve and the corresponding minimum is the saturation point. The changes of the effective nucleon mass M^* to ρ_B are

shown in Fig.9a and Fig.9b where the curves in Fig.9a limit to the low density region ($0 \text{ fm}^{-3} \leq \rho_B \leq 0.20 \text{ fm}^{-3}$), and curves in Fig.9b cover a large density region. We find that M^* decreases when density and/or temperature increases. This result is similar to the of QMC model[47] and Walecka model. At the saturation point, $M^*/M = 0.6$, as indicated.

IV. SUMMARY

In summary, we present an extended quark mass density- and temperature- dependent model which is motivated by the QMDTD model and the quark meson coupling model. The σ and ω fields are assumed to couple with the u, d quarks. The MIT boundary constrain has been given up and the non-permanent quark confinement mechanism is mimicked by the quark mass density- and temperature- dependence. It is shown that under mean field approximation this model provides a reasonable description of the saturation properties for nuclear matter in the region of low temperature and density. While at sufficient high temperature and/or density, the deconfinement phase transition takes place automatically. The phase transition is characterized by that the bag radius tends to infinite and the effective baryon mass M^* vanishes simultaneously. The deconfinement phase diagram which has the same behavior as that of lattice QCD calculation is addressed. We emphasize that in our calculation the deconfinement process is treated consistently within one unified model. This is different from the usual investigation which employs two separate models to describe respectively the hadronic phase and quark gluon plasma phase, and use the Gibbs conditions to determine the phase diagram[26,27].

Acknowledgments

This work is supported in part by National Natural Science Foundation of China under No.10375013, 10405008, 10247001, 10235030, National Basic Research Program of China 2003CB716300, and the Foundation of Education Ministry of China 20030246005.

[1] P.A.M. Guichon, Phys. Lett. B200 (1988) 235

- [2] K. Saito and A.W. Thomas, Phys. Lett. B327 (1994) 9, Phys. Lett. B335 (1994) 17, Phys. Rev. C52 (1995) 2789
- [3] X. Jin and B.K. Jennings, Phys. Rev. C54 (1996) 1427, Phys. Lett. B374 (1996) 13
- [4] H.Q. Song and R.K. Su, Phys. Lett. B358 (1995) 179
- [5] I. Zakout, H.R. Jaqaman, S. Pal, H. Stöcker and W. Greiner, Phys. Rev. C61 (2000) 055208
- [6] P. Wang, R.K. Su, H.Q. Song and L.L. Zhang, Nucl. Phys. A653 (1999) 166
- [7] H.Q. Song, R.K. Su, D.H. Lu and W.L. Qian, Phys. Rev. C68 (2003) 055201
- [8] P.K. Panda, G. Krein, D.P. Menezes and Providencia, Phys. Rev. C68 (2003) 015201
- [9] G.N. Fowler, S. Raha and R.M Weiner, Z. Phys. C9 (1981) 271
- [10] O.G. Benvenuto and G. Lugones, Phy. Rev. D51 (1995) 1989, G. Lugones and O.G. Benvenuto, Phy. Rev. D52 (1995) 1276
- [11] Y. Zhang and R.K. Su, Phys. Rev. C 67 (2003) 015202
- [12] Y. Zhang, R.K. Su, S.Q. Ying, and P. Wang, Europhys. Lett. 56 (2001) 361;
- [13] Y. Zhang and R.K. Su, Phys. Rev. C 65 (2002) 035202;
- [14] Y. Zhang and R.K. Su, Mod. Phys. Lett A18 (2003) 143
- [15] Y. Zhang and R.K. Su, Jour. Phys. G30 (2004) 811
- [16] C. Wu, W.L. Qian and R.K. Su, Phys. Rev. C (in press)
- [17] J.Y. Shen, Y. Zhang, B. Wang and R.K. Su, Int. J. Mod. Phys. A (in press)
- [18] V.K. Gupta, A. Gupta, S. Singh and J.D. Anand, Int. J. Mod. Phys. D12 (2003) 583
- [19] Z.X. Qian, C.G. Su and R.K. Su, Phys. Rev. C47 (1993) 877
- [20] R.K. Su, G.T. Zheng and G.G. Siu, J. Phys. G19 (1993) 79
- [21] W.L. Qian, R.K. Su and P. Wang, Phys. Lett. B491 (2000) 90
- [22] Z.Y. Ma, J. Rong, B.Q. Chen, Z.Y. Zhu and H.Q. Song, Phys. Lett. B604 (2004) 170
- [23] Y.H. Tan, H. Shen, P.Z. Ning, Phys. Rev. C63 (2001) 055203
- [24] L.L. Zhang, H.Q. Song, P. Wang and R.K. Su, J. Phys. G26 (2000) 1301
- [25] R.J. Furnstahl, B.D. Serot and H.B. Tang, Nucl. Phys. A615 (1997) 441
- [26] K.S. Lee and U. Heinz, Phys. Rev. D47 (1993) 2068
- [27] H. Müller, Nucl. Phys. A618 (1997) 349

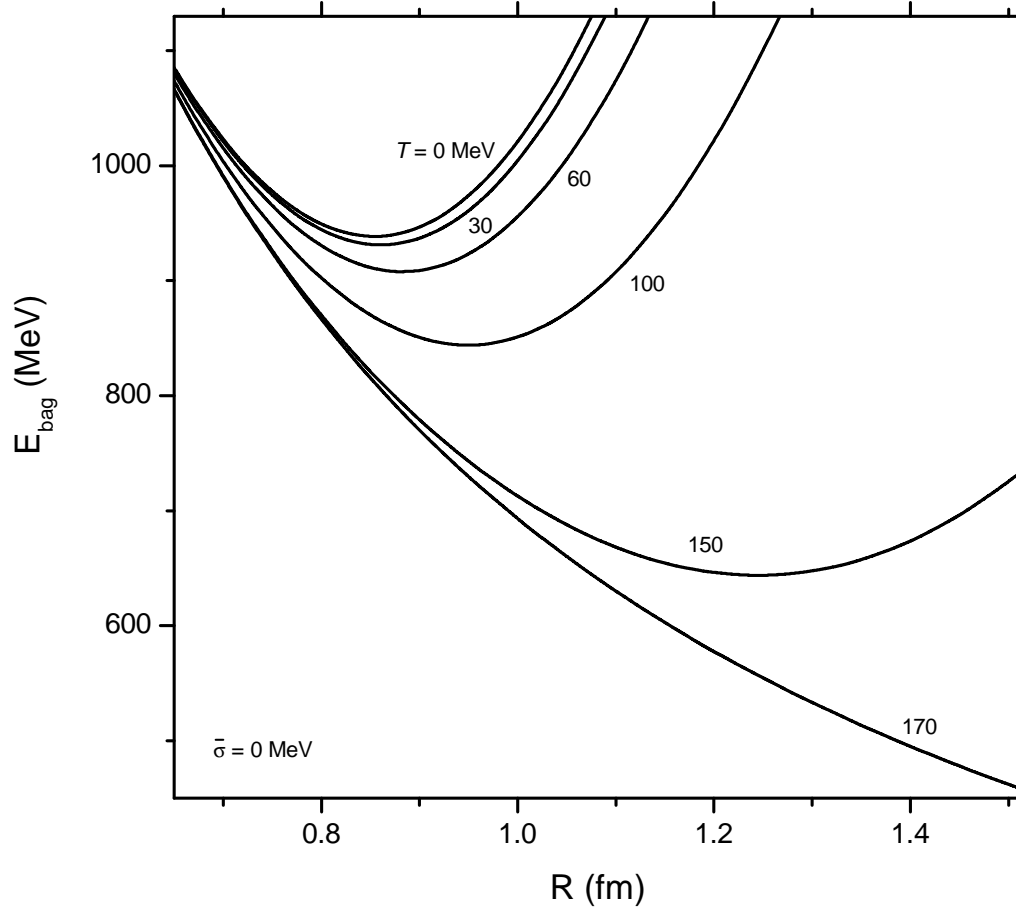


Fig. 1a

FIG. 1: The bag energy as a function of bag radius without meson at different temperatures $T = 0, 30, 60, 100, 150$ and 168 MeV, with $\bar{\sigma} = 0$ MeV, the radius for nucleon is determined by the minimum of bag energy.

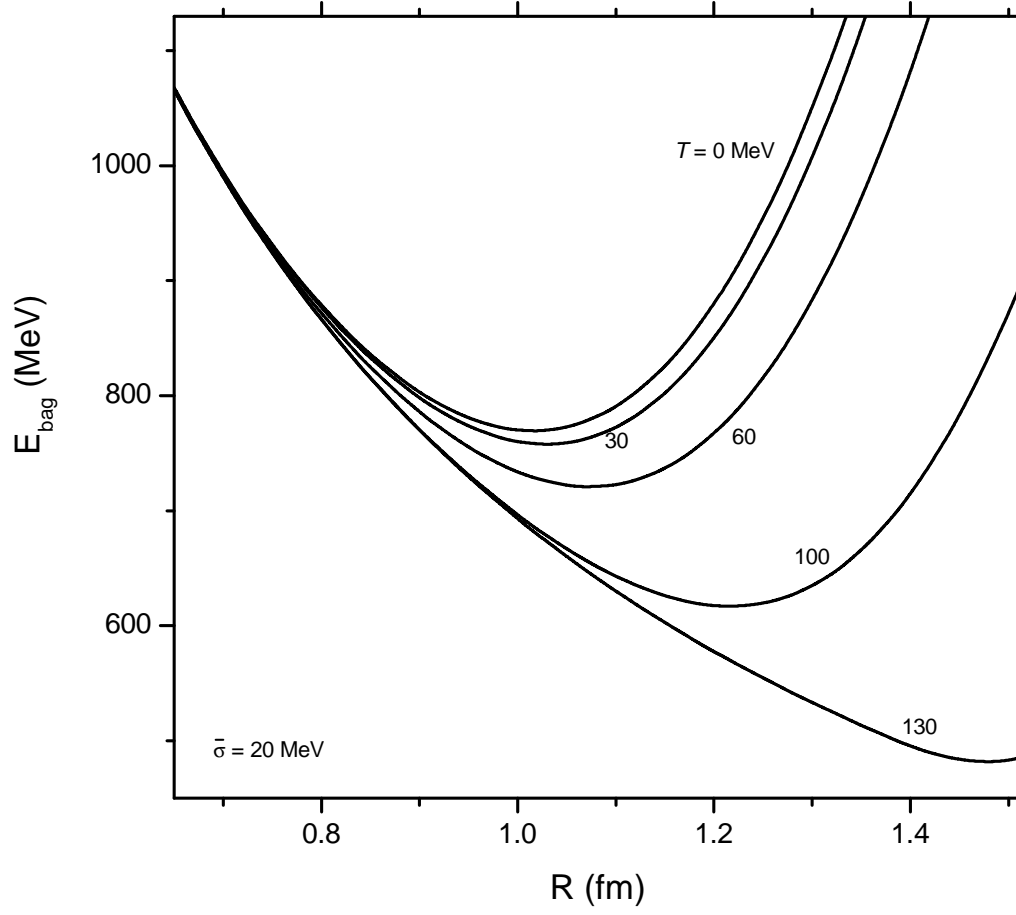


Fig. 1b

FIG. 2: The bag energy as a function of bag radius without meson at different temperatures $T = 0, 30, 60, 100, 150$ and 170 MeV, with $\bar{\sigma} = 20$ MeV.

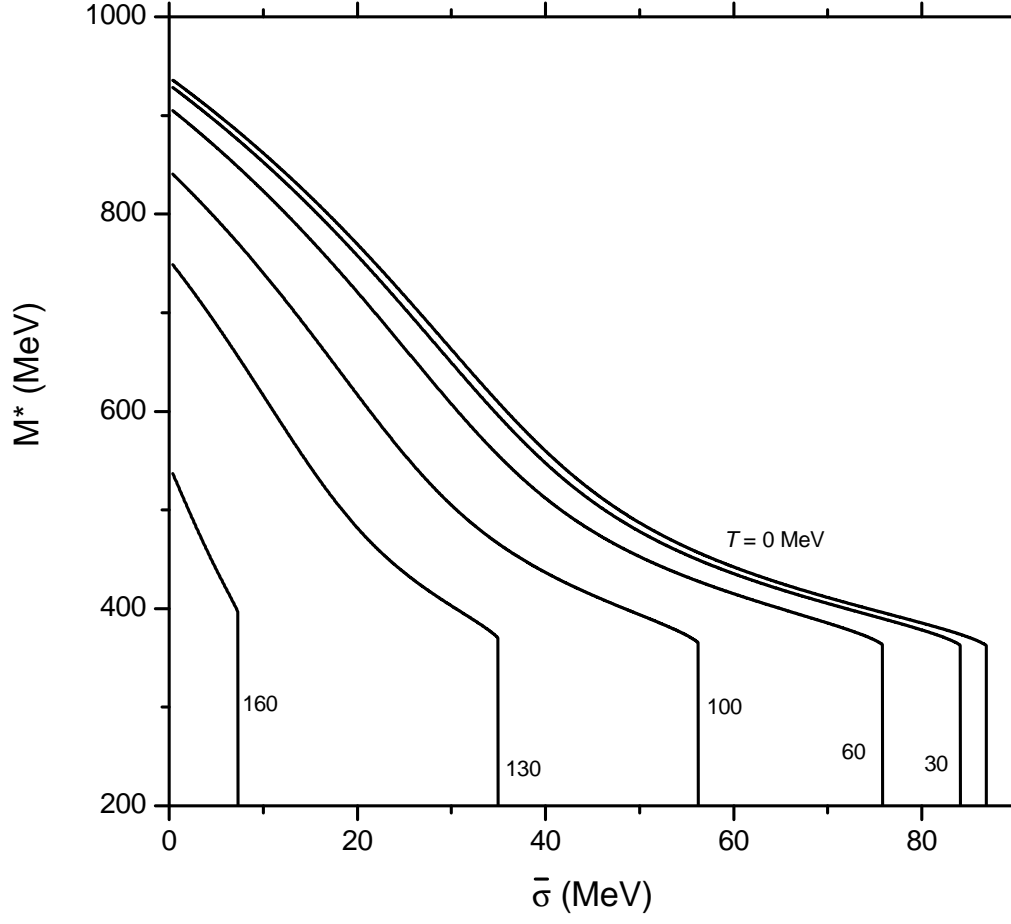


Fig.2

FIG. 3: Effective nucleon masses vs. the $\bar{\sigma}$ at different temperatures $T = 0, 30, 60, 100, 130$ and 160 MeV respectively

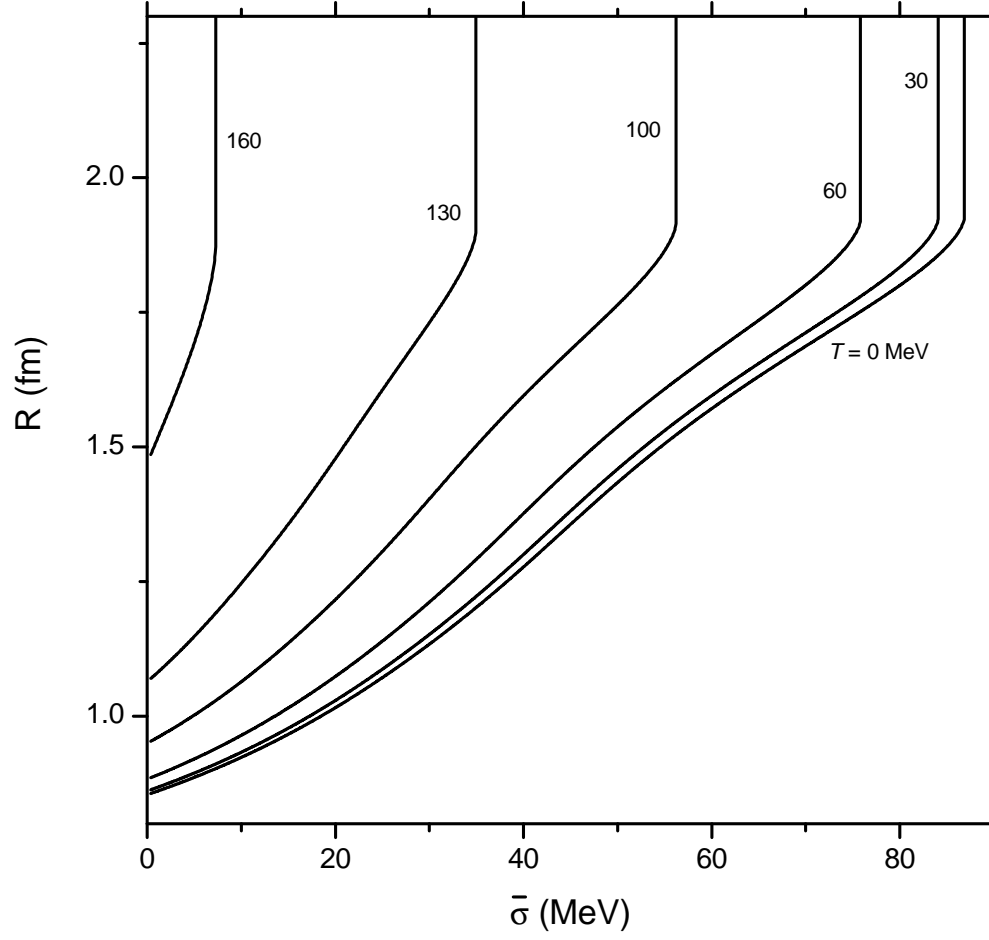


Fig.3

FIG. 4: Nucleon radius vs. the $\bar{\sigma}$ at different temperatures $T = 0, 30, 60, 100, 130$ and 160 MeV respectively

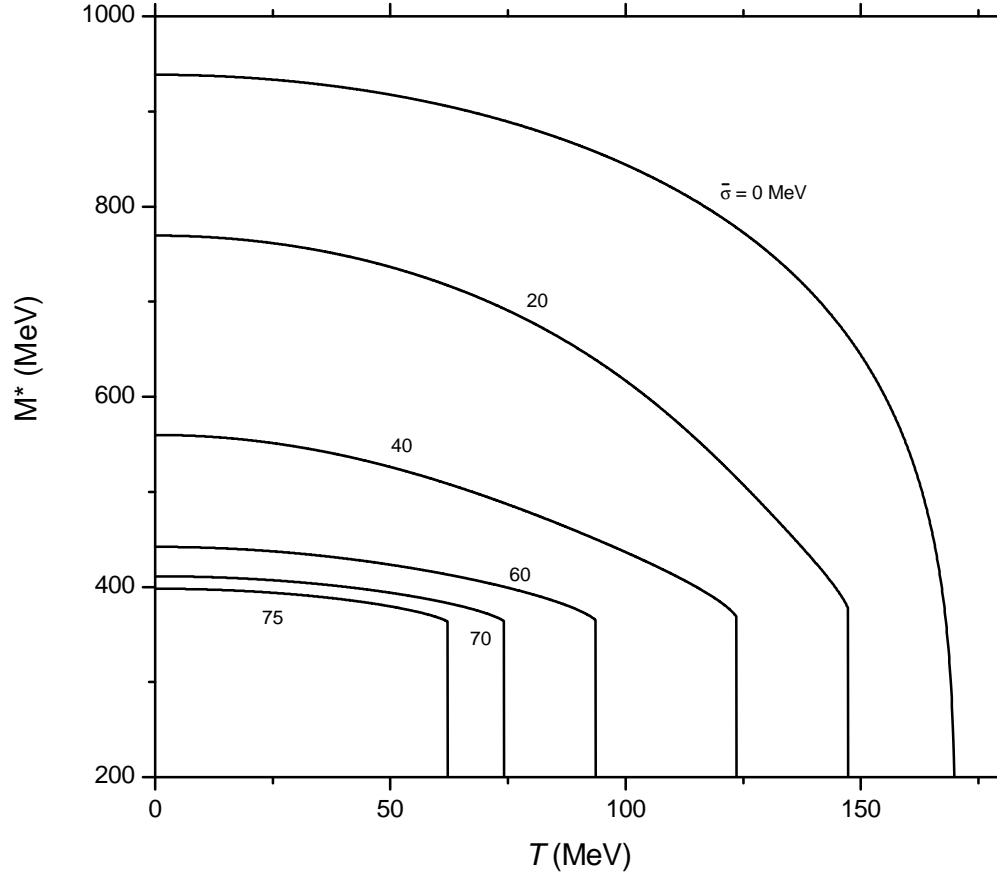


Fig.4

FIG. 5: Effective nucleon masses vs. the temperatures at different values $\bar{\sigma} = 0, 20, 40, 60, 70$ and 75 MeV respectively

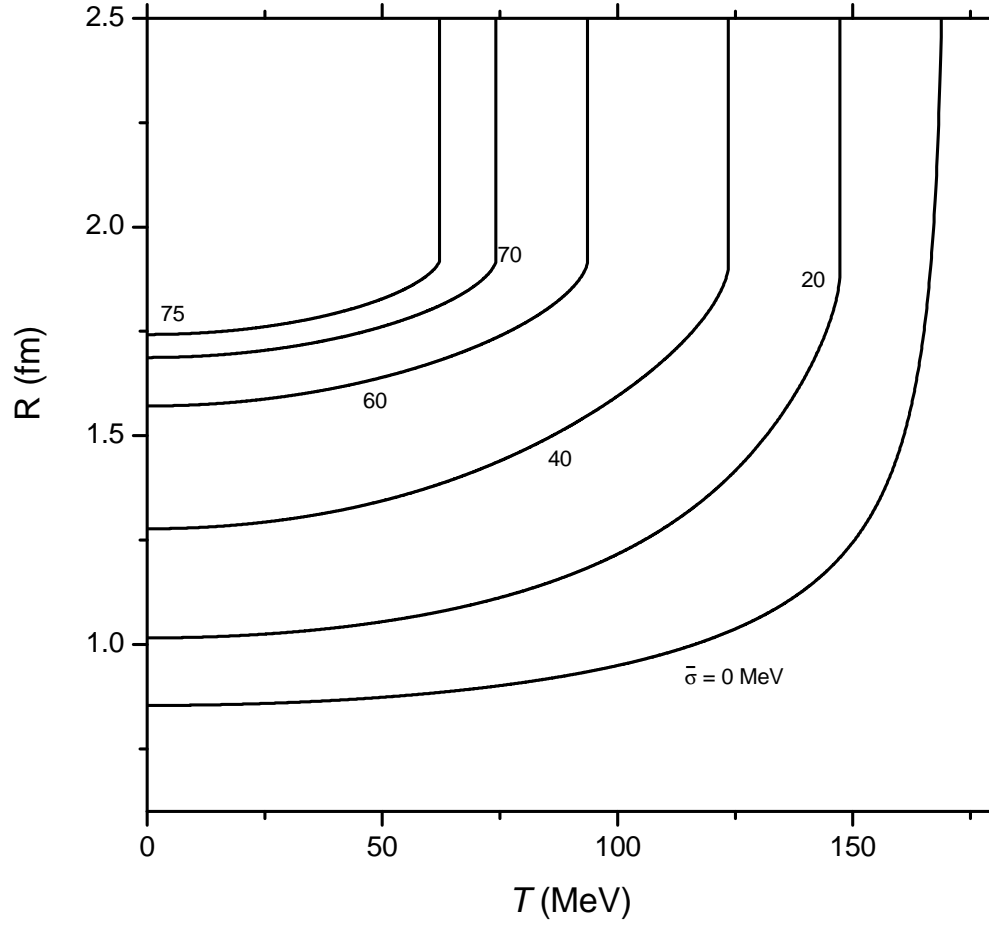


Fig.5

FIG. 6: Nucleon radius vs. the temperatures at different values $\bar{\sigma} = 0, 20, 40, 60, 70$ and 75 MeV respectively

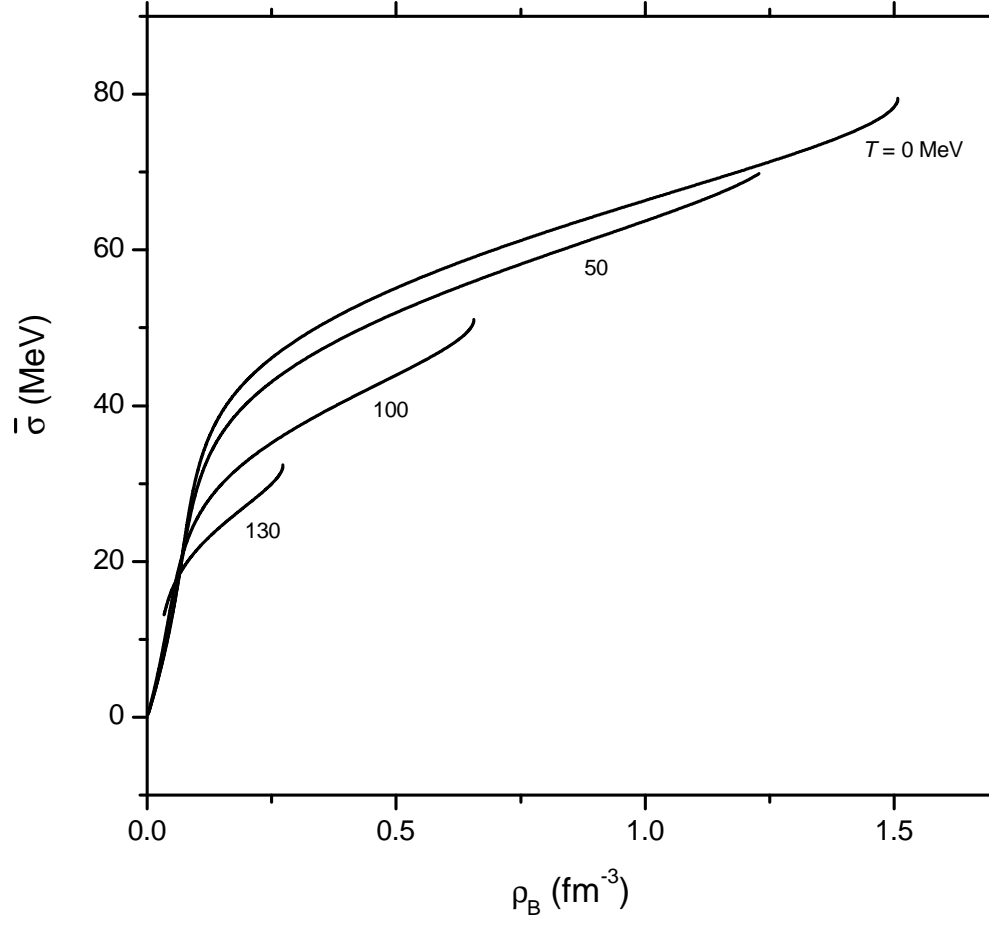


Fig.6

FIG. 7: $\bar{\sigma}$ vs. baryon density ρ_B at different temperatures $T = 0, 50, 100$ and 130 MeV respectively

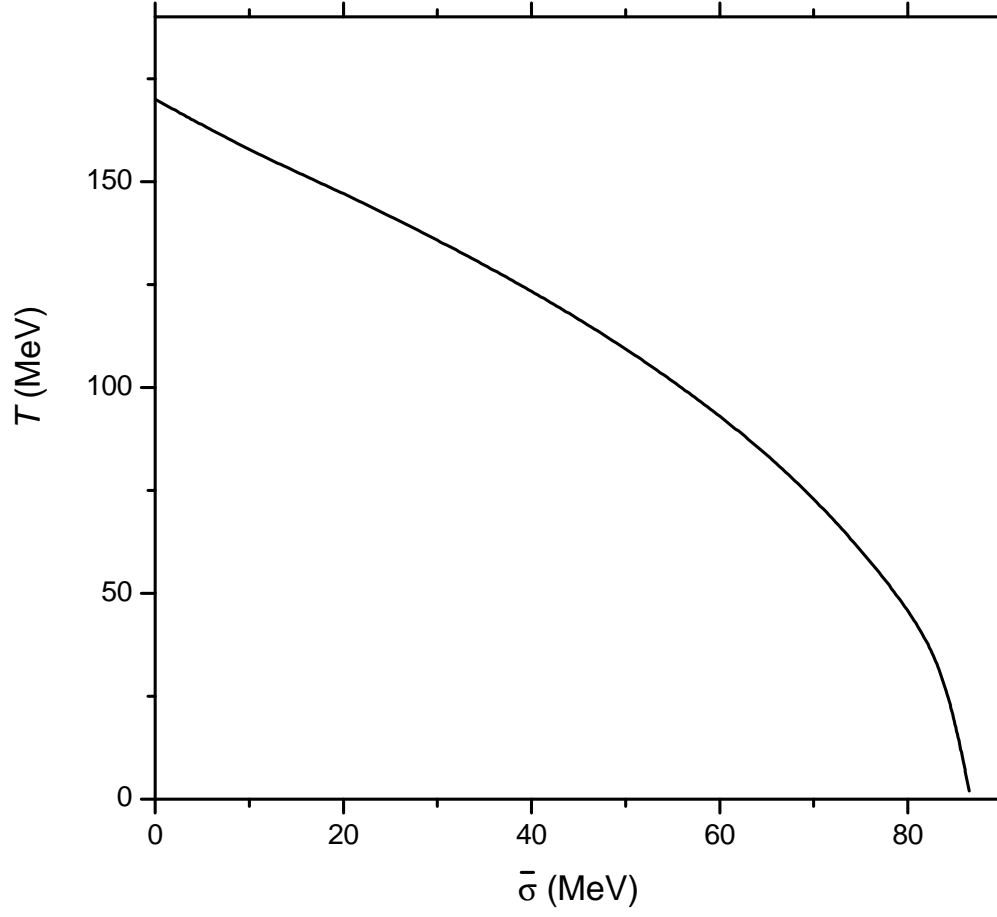


Fig.7

FIG. 8: Critical temperature of deconfinement transition t_c vs. $\bar{\sigma}$

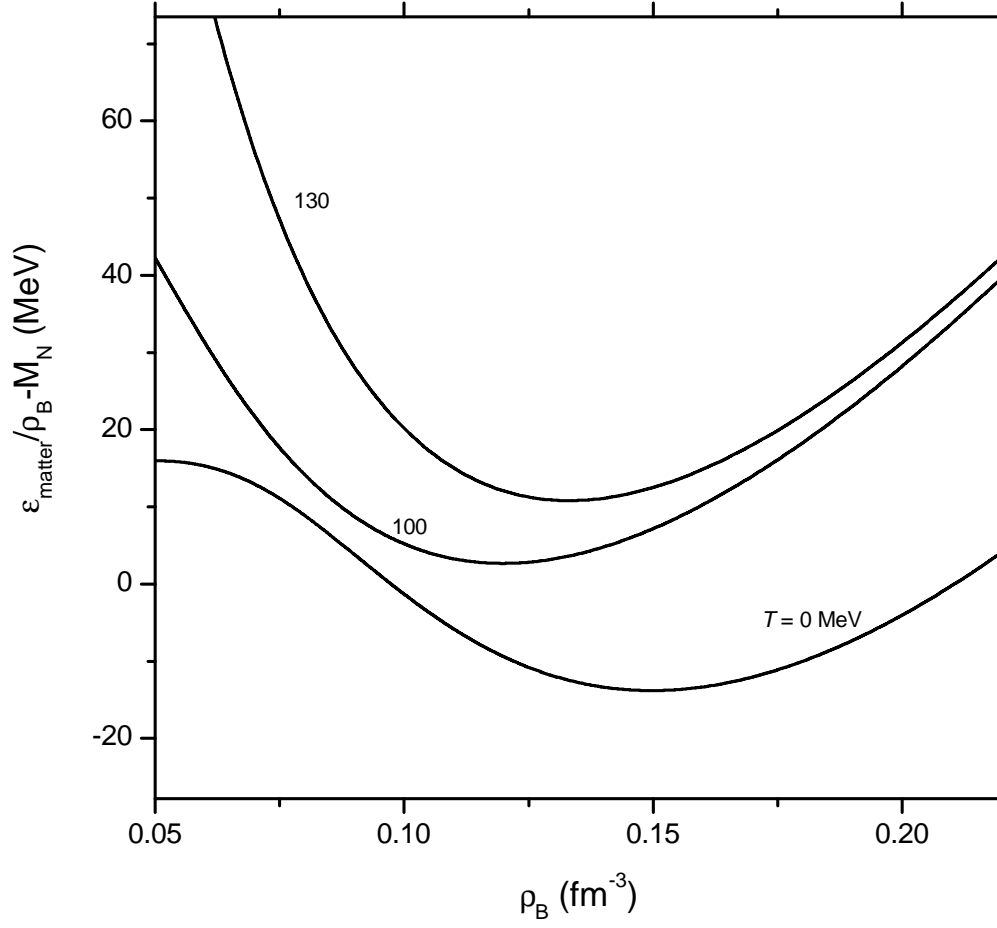


Fig.8

FIG. 9: Saturation curve of nuclear matter at different temperatures $T = 0, 100$ and 130 MeV respectively

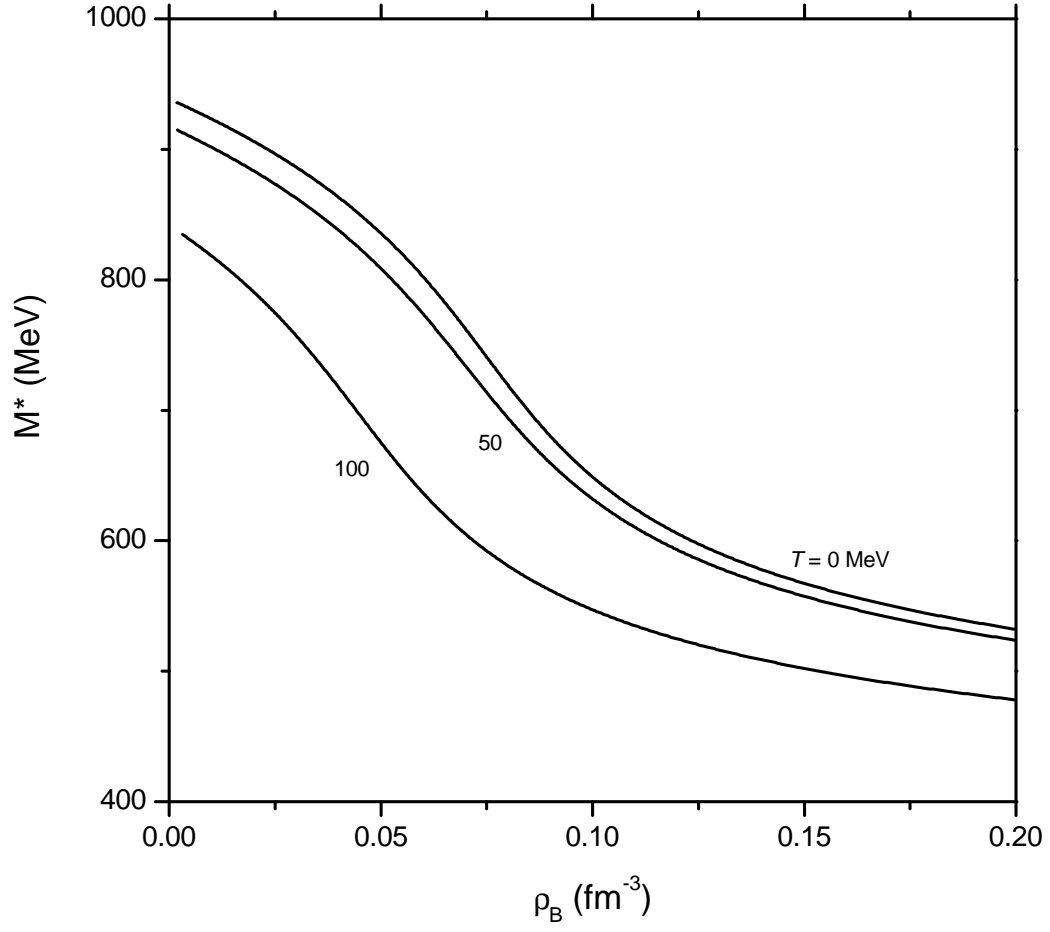


Fig.9a

FIG. 10: Effective nucleon mass vs. baryon density at different temperatures $T = 0, 50$ and 100 MeV respectively

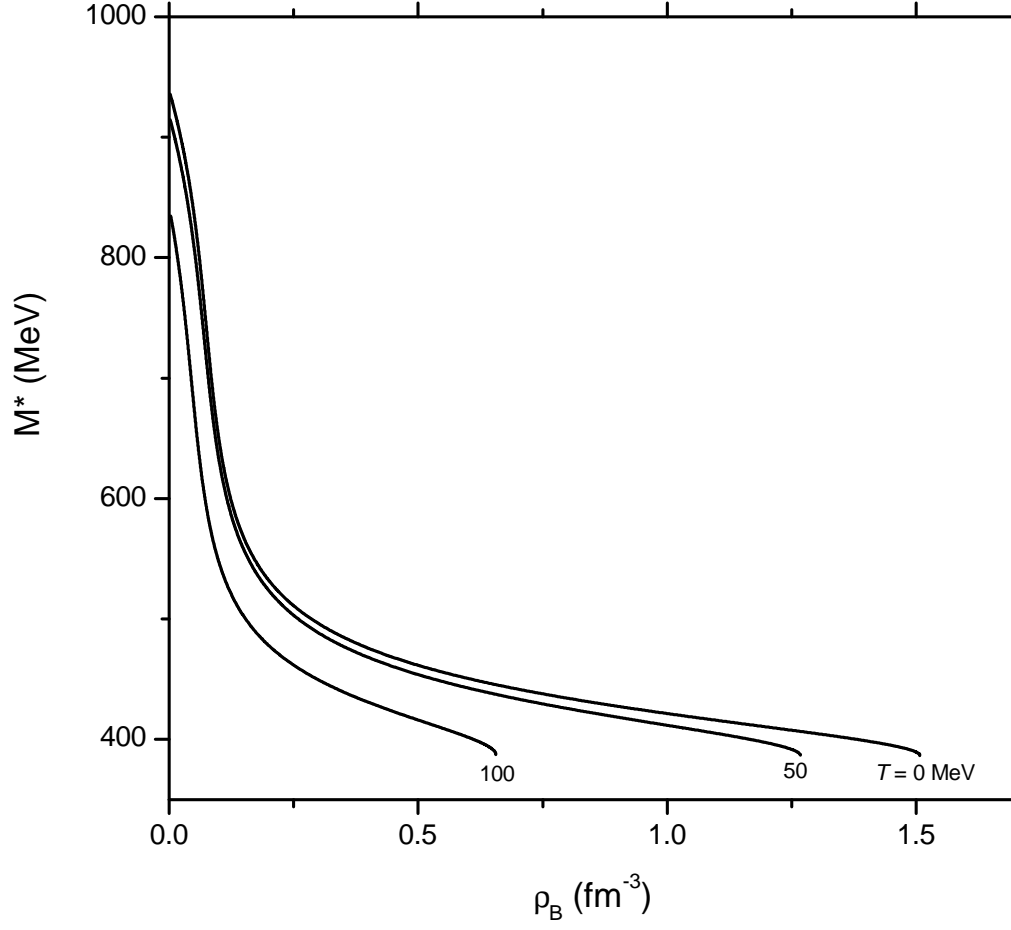


Fig.9b

FIG. 11: The same curve as Fig.4b with a wider range of baryon density at different temperatures $T = 0, 50$ and 100 MeV respectively